Nuclear localization of dirhodium(II) complexes in breast cancer cells by X-ray fluorescence microscopy

Alejandra Enriquez Garcia,[a] Barry Lai,[b] Sesha Gopal Gopinathan,[c] Hugh H. Harris,[d] Carrie S. Shemanko,[c] and Farideh Jalilehvand*[a]

a) *Department of Chemistry, University of Calgary, Calgary, AB T2N 1N4, Canada.*

b) *Advanced Photon Source, X-ray Science Division, Argonne National Laboratory, Argonne, IL 60439, USA.*

c) *Department of Biological Sciences, University of Calgary, Calgary, AB T2N 1N4, Canada.*

d) *Department of Chemistry, The University of Adelaide, SA 5005, Australia.*

Abstract. The cellular distribution of three dirhodium(II) complexes with paddlewheel structure was investigated using synchrotron-based X-ray fluorescence microscopy and cell viability studies. Complexes with vacant axial sites, displayed cytotoxic activity and nuclear accumulation whereas the complex in which the axial positions are blocked showed little to no toxicity nor uptake.

The use of metal complexes for the treatment of breast cancer has been extensively investigated in the last decades.[1, 2] Triple-negative breast cancer (TNBC) patients usually have poor prognosis due to the aggressiveness of TNBC and lack of targeted therapy,[3-5] making research in this area imperative. In addition to platinum-based drugs, which have shown promising effects,[6-8] complexes of other metals including ruthenium,[9-11] osmium,[12] rhodium,[13, 14] and palladium[15] have also captured interest.

Dirhodium(II) species have displayed remarkable anticancer activities in different cancer cell lines, in some cases comparable to cisplatin.[16] These complexes have been shown to bind covalently to DNA bases, preferentially purines,[17] nucleotides,[18-20] as well as single- and double-stranded DNA.[21] This binding to DNA is believed to initially occur via the axial sites of these dirhodium(II) complexes, followed by a shift to the equatorial positions.[22-25] It would then be expected that strong, non-labile axial ligands would decrease the cytotoxicity of such complexes. It was reported that DNA binding as well as inhibition of DNA transcription decreased significantly from *cis*-$[Rh_2(AcO)_2(np)_2]^{2+}$ (np = 1,8-napthyridine) with vacant axial sites, to *cis*-$[Rh_2(AcO)_2(pynp)_2]^{2+}$ (pynp = 2-(2-pyridyl)-1,8-naphthyridine) with blocked axial positions.[26]

Apart from this potential DNA-based mode of action, the interactions of dirhodium(II) complexes with other biomolecules such as proteins and enzymes have also been studied.[27-29] Siu and coworkers proposed a different mechanism of action involving the inhibition of the ubiquitin–proteasome system (UPS).[30] For a series of dirhodium(II) carboxylates, the authors reported that the concentrations needed to inhibit UPS were 10-fold lower than those required for DNA damage, suggesting this mechanism would predominate in cells.[30] However, the specific cellular targets for these complexes are yet to be elucidated.[31]

In an effort to identify the subcellular targets for these dirhodium(II) complexes, Peña *et al.* tethered a green fluorescent bodipy moiety (4,4-difluoro-4-bora-3a,4a-diaza-*s*-indacene) to a dirhodium(II) to monitor its accumulation in lung cancer cells (A459) using confocal fluorescence microscopy.[32] Contrary to the expected nuclear accumulation, colocalization experiments with lysosome- and mitochondria-specific fluorescent trackers revealed that the fluorophore-containing complex was

localized both in the mitochondria and lysosomes, with a slight preference for the latter.[32] The absence of accumulation in the nucleus was explained as due to the influence of the bodipy fluorophore on the biological properties and subcellular localization of the dirhodium(II) complex. Minus and coworkers reported the preparation of dirhodium(II) carboxy-fluorophore conjugates to assess the intracellular fate of dirhodium(II) complexes. Their studies revealed that the cellular permeability of the dirhodium(II)-fluorophore moiety improves the cellular uptake of the fluorophore agent, and the dirhodium(II) scaffold can act as "turn on" imaging agent by releasing the fluorophore upon complex decomposition inside the cell.[33]

In this regard, X-ray fluorescence microscopy (XFM) poses an advantage as it relies on the intrinsic fluorescence of the individual elements rather than the presence of fluorophores (Scheme S1). This technique has been exploited due to its high sensitivity and sub-micrometer spacial resolution to determine cellular uptake as well as intracellular distribution for a variety of compounds, including Cr(VI),[34] As,[35] Pt,[36] Os,[37] as well as Ru complexes in cancer cells[38] (for an in-depth review, see Ref. 39). Recently, Markham *et al.* reported the Rh elemental maps collected using XFM on lung cancer cells treated with complexes [Rh(*Cp)Cl(acac)] (acac = acetylacetonato, *Cp = pentamethylcyclopentadienato) and [Rh(*Cp)Cl(cur)] (curH = curcumin) as potential curcumin delivery drugs; however, no specific localization was observed for Rh inside the cells.[40]

In this study, we report the cytotoxicity, cellular uptake and biodistribution of three different dirhodium(II) complexes: $Rh_2(AcO)_4$ (**1**), $[Rh_2(AcO)_2(Met)_2]\cdot 5H_2O$ (**2**, HMet = methionine) and $[Rh_2(AcO)_2(bpy)_2](AcO)_2$ (**3**, bpy = 2,2'-bipyridine) (Figure 1).[41] By comparing the results for **1** and **2**, we will be able to evaluate whether axial vacancies are essential for the cytotoxicity and cellular uptake of these complexes. Complex **3** was selected for comparison due to its higher water solubility relative to **1**.[42] This represents the first study of its kind to investigate the uptake and cellular distribution of several dirhodium(II) complexes that does not involve the covalent incorporation of a fluorophore, which has shown to affect subcellular distribution.[32] Since the ability of these complexes to traverse the plasma membrane seems critical for their activity,[31] evaluating the uptake using XFM will provide a better understanding of the structure-activity relationship of these complexes and the necessary characteristics to optimize drug design.

In order to determine the cell toxicity of these complexes, cell viability studies were performed on the breast cancer cell line MDA-MB-231 (for details, see *Electronic Supplementary Information* (ESI)). These experiments showed that complex **2**, without vacant axial sites, had no toxicity even at concentrations in the mM range (Table 1, and Figures S7 and S8). This suggests, as hypothesized previously,[26] that vacancies in the axial positions are necessary for the dirhodium(II) complex to be cytotoxic. Complexes **1** and **3** displayed higher cytotoxicity than **2**, but still inferior than cisplatin under the same 48-hour timeframe (Table 1).[43] Interestingly, although the water solubility of **3** is significantly higher than **1**, it did not improve the cytotoxicity. This lower cytostatic activity of **3** in comparison to **1** was previously observed on the human oral carcinoma KB cell line.[44]

For the XFM imaging experiments, cells were treated for 6 hours with 200 μM solutions of complexes **1**-**3** in DMEM. For comparison, the control cells were treated with DMEM only. The 6-hour timeline was chosen to maximize drug uptake while minimizing drug efflux from the cell (see *ESI*). The experiments were performed at 23.8 KeV to obtain the Rh distribution maps and repeated on the same cells at 12.8 KeV to enhance the signal of the lighter elements (P through Zn). The XFM images for the control and the treated cells are shown in Figures 2 and S9-S12.

In the control cells, the rhodium concentration was very low with no specific localization (Figure S9); however, some residual signal was detected (see quantification in Figure S13). This signal is an artifact

of the fitting procedure as can be observed by the lack of a peak for the Rh Kα fluorescence (20.2 KeV) in the experimental XFM spectrum (Figure S14). When cells were treated with **1**, the maps obtained at high energy (23.8 KeV) as compared to those at lower energy (12.8 KeV) revealed Rh colocalization with the distribution of P and Zn in the cells (Figure 2 *top* and Figure S10). Both P and Zn are known to exhibit high nuclear concentration due to its presence in

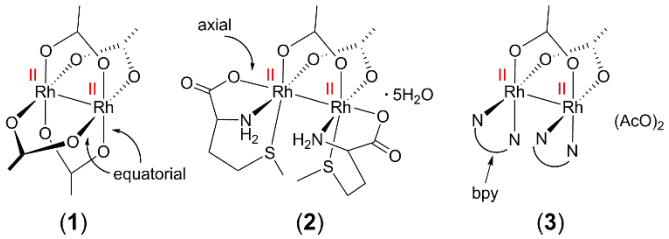

Figure 1 Structures of $Rh_2(AcO)_4$ (**1**), $[Rh_2(AcO)_2(Met)_2]\cdot 5H_2O$ (**2**) and $[Rh_2(AcO)_2(bpy)_2](AcO)_2$ (**3**).

Table 1 Cytotoxicity of Complexes 1-3 for MDA-MB-231 Breast Cancer Cells Determined from the Alamar Blue Assay and Their Comparison with Cisplatin

Complex	**IC_{50} / μM**
$Rh_2(AcO)_4$ (**1**)	40 ± 2.4
$[Rh_2(AcO)_2(Met)_2]\cdot 5H_2O$ (**2**)	> 1000
$[Rh_2(AcO)_2(bpy)_2](AcO)_2$ (**3**)	315 ± 79
Cisplatin	23.0 [a]

[a] Ref. 43. See cytotoxicity graphs in Figures S7 and S8.

the DNA backbone and zinc finger proteins, respectively.[45] The optical micrographs were also employed to confirm the location of the nucleus in the cells. Similar distribution was observed when cells were treated for 1 hour (Figure S15). Quantification of the total average rhodium content was calculated for the nuclear region and the whole cell to estimate the percentage of Rh accumulated in the nucleus (Figure S13). The average (n=4) nuclear rhodium content for cells treated with **1** was estimated at 39.6 % of the total intracellular rhodium (Table S1), which showcases great affinity for the nucleus.

When cells were treated with the non-toxic complex **2** using the same concentration, treatment time and data collection parameters (i.e. dwell time and step size), very little Rh content was detected in the elemental maps (Figure 2 *middle* and Figure S11). Quantification of the Rh content revealed no significant increase in cellular and nuclear Rh content compared to the control (Figure S13). Moreover, the XFM spectrum shows no peak detected for the Rh Kα fluorescence (Figure S14). This suggests that the limited cytotoxicity of complex **2** (IC_{50} > 1 mM; Table 1) might be a result of the poor uptake of this complex by the cells due to its blocked axial positions.

For cells treated with complex **3**, the corresponding Rh distribution maps overlap mainly with the P and Zn maps, as was observed for complex **1** (Figure 2 *bottom* and Figure S12). In this case, the percentage of nuclear to intracellular content of rhodium was 39.1 %, which is similar to that observed for **1** (39.6%), suggesting similar nuclear affinity (Figure S13 and Table S1). For this treatment, some extracellular rhodium signal was detected suggesting a potential affinity of this complex for the silicon

nitride windows; a similar effect was observed with a rhenium(I) tricarbonyl tetrazolato complex.[46] Although complex **3** has higher water solubility relative to **1**, there is no significant difference between the Rh content for cells treated with compounds **1** and **3**, suggesting that uptake is not affected by the water solubility of these complexes. This alongside the poorer cytotoxicity of **3** with respect to **1** (Table 1) indicates that although complex **3** is taken up by the cells in a similar amount as **1** (Table S1), its intracellular effect is much less harmful, thus suggesting differences in their potency. We are uncertain about the exact reasons behind this, but we speculate it might be due to the 2,2'-bipyridine ligand acting as a poor leaving group, or the limited ability of **3** to act as a DNA intercalator as an alternative mechanism.[31, 47]

In order to assess whether polarity of the complexes would affect their cellular uptake, we performed density functional theory calculations on **1-3** to evaluate the dipole moment. The calculated dipole moment in gas phase increased in **1** < **2** < $[Rh_2(AcO)_2(bpy)_2]^{2+}$ with the latter being the most polar (least lipophilic). This trend does not correlate with the uptake of these complexes, however since the polarity may change in cell media, its influence remains uncertainThe homeostasis of the lighter

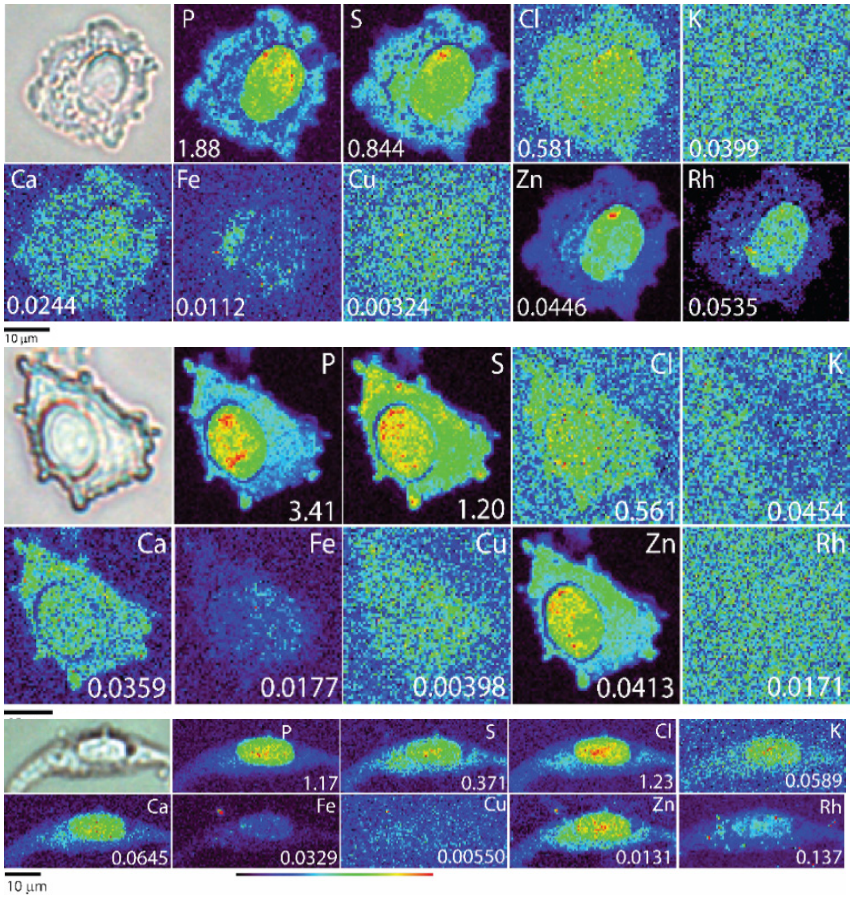

Figure 2 Optical micrographs (*top left*), and XFM elemental distribution maps of P, S, Cl, K, Ca, Fe, Cu, Zn, and Rh of MDA-MB-231 cells treated for 6h with 200 µM solutions of *top*) $Rh_2(AcO)_4$ (**1**), *middle*) $[Rh_2(AcO)_2(Met)_2]\cdot 5H_2O$ (**2**) and *bottom*) $[Rh_2(AcO)_2(bpy)_2](AcO)_2$ (**3**) in DMEM. Maximal elemental area density (in µg/cm^2) is given in the bottom corner of each map.

elements did not seem to be majorly disrupted by the treatment with compounds **1-3** (see Figure S13). Only the intracellular content of copper and iron seemed to significantly increase upon treatment with the dirhodium(II) drugs. An increase in copper content has been observed previously when lung cancer cells (A459) were treated with Se-containing compounds, including selenomethionine and selenite.[48, 49] This was ascribed to an upregulation of Cu,Zn-superoxide dismutase (SOD1) as a response to

increased levels of reactive oxygen species (mainly $O_2^{\cdot-}$), generated by selenite.[48, 50] Recent studies have shown that upon aerobic reaction of an aqueous solution **1** with thiol-containing biomolecules such as glutathione, production of peroxide species was detected.[27, 51] Therefore, a potential pathway involving the production of reactive oxygen species cannot be ruled out.

In the case of iron, intracellular levels increased for all three treatments, indicating a specific relationship between iron levels and dirhodium(II) complexes. In comparison, no statistically significant change was observed in the cellular iron content of cells treated with the ruthenium-based KP1019 drug, *trans*-[$Ru^{III}(Ind)_2Cl_4$][IndH] (Ind = indazole), but its distribution changed (relative to the control cells), with Fe and Ru only partially colocalized proximate to the nucleus.[38, 52] It has been shown that the delivery of KP1019 into the cell is considerably enhanced when it is bound to Fe(III) loaded-transferrin, making it easier for the transferrin receptors on the cell surface to recognize the protein.[52] So, perhaps the possibility of transporting dirhodium(II) complexes by iron binding proteins could be considered in future. Recently, Yang *et al.* have reported how $Rh_2(AcO)_4$ (**1**) can be taken up by bacteria via the PiuABCD haem-uptake system and interfere with iron metabolism in *S. pneumoniae*, leading to bacterial cell death.[53]

The results presented herein confirm that $Rh_2(AcO)_4$ (**1**) preferentially accumulates in the nucleus of breast cancer MDA-MB-231 cells. This is the first example in which the biodistribution of this complex, without any chemical modification, has been monitored inside cells. This finding suggests that nuclear DNA is the ultimate target for this family of complexes. Unlike **1**, our recently synthesized $[Rh_2(AcO)_2(Met)_2]\cdot 5H_2O$ complex (**2**) with blocked axial sites,[41] was not taken up by the cells as evidenced by a non-significant increase in intracellular Rh content (relative to the controls) and lack of specific cellular localization. This confirms a previous hypothesis that vacant axial positions are essential for both uptake and cytotoxicity of dirhodium(II) complexes.[26] The comparison between **1** and **3**, with two 2,2'-bipyridine as equatorial ligands and improved water solubility, revealed that although uptake is similar in both cases, **3** seems to be a much less potent anticancer drug, as demonstrated by its higher IC_{50} value. Results from this investigation provide a better picture of the intracellular fate and potential main targets of dirhodium(II) complexes in cancer cells, highlighting the importance of vacant axial positions for their delivery into the cell. This study can be of high interest in the strategic design of more active anticancer therapeutics, showing that synchrotron-based X-ray fluorescence microscopy is a very powerful tool capable of providing key information about the uptake and biodistribution of dirhodium(II) complexes inside cancer cells.

The authors acknowledge financial support from the Natural Science and Engineering Research Council of Canada (NSERC) funding reference number RGPIN 2016-04546 (FJ) and RGPIN-2018-04773 (CS), the Canadian Foundation for Innovation (CFI), the Province of Alberta (Department of Innovation and Science) and the Canadian Cancer Society (#300072). X-ray fluorescence microscopy data collection was carried out at the Advanced Photon Source (Proposal No. 53103). Use of the Advanced Photon Source was supported by the U. S. Department of Energy, Office of Science, Office of Basic Energy Sciences, under Contract No. DE-AC02-06CH11357. H.H.H. acknowledges travel funding provided by the International Synchrotron Access Program (ISAP) managed by the Australian Synchrotron, part of ANSTO, and funded by the Australian Government.

Conflicts of interest

There are no conflicts to declare.

Notes and references

1. E. M. Domínguez-Martís, D. G. Mosteiro-Miguéns, L. Vigo-Gendre, D. López-Ares, *et al.*, *Crystals*, 2018, **8**, 369.
2. A. Bergamo, G. Sava, *Chem. Soc. Rev.*, 2015, **44**, 8818-8835.
3. C. K. Anders and L. A. Carey, *Clin. Breast Cancer*, 2009, **9**, S73-S81.
4. L. Malorni, P. B. Shetty, C. De Angelis, S. Hilsenbeck, *et al.*, *Breast Cancer Res. Treat.*, 2012, **136**, 795-804.
5. G. Bianchini, J. M. Balko, I. A. Mayer, M. E. Sanders and L. Gianni, *Nat. Rev. Clin. Oncol.*, 2016, **13**, 674.
6. D. P. Silver, A. L. Richardson, A. C. Eklund, Z. C. Wang, *et al.*, *J. Clin. Oncol.*, 2010, **28**, 1145-1153.
7. F. André and C. C. Zielinski, *Ann Oncol.*, 2012, **23**, vi46-vi51.
8. S. J. Isakoff, E. L. Mayer, L. He, T. A. Traina, *et al.*, *J. Clin. Oncol.*, 2015, **33**, 1902-1909.
9. C. P. Popolin, J. P. B. Reis, A. B. Becceneri, A. E. Graminha, *et al.*, *PLOS ONE*, 2017, **12**, e0183275.
10. M. Frik, A. Martínez, B. T. Elie, O. Gonzalo, *et al.*, *J. Med. Chem.*, 2014, **57**, 9995-10012.
11. T. Nhukeaw, P. Temboot, K. Hansongnern and A. Ratanaphan, *BMC Cancer*, 2014, **14**, 73.
12. K. Suntharalingam, W. Lin, T. C. Johnstone, P. M. Bruno, Y.-R. Zheng, M. T. Hemann and S. J. Lippard, *J. Am. Chem. Soc.*, 2014, **136**, 14413-14416.
13. G.-J. Yang, H.-J. Zhong, C.-N. Ko, S.-Y. Wong, K. Vellaisamy, M. Ye, D.-L. Ma and C.-H. Leung, *Chem. Commun.*, 2018, **54**, 2463-2466.
14. G.-J. Yang, W. Wang, S. W. F. Mok, C. Wu, B. Y. K. Law, X.-M. Miao, K.-J. Wu, H.-J. Zhong, C.-Y. Wong, V. K. W. Wong, D.-L. Ma and C.-H. Leung, *Angew. Chem. Int. Ed.*, 2018, **57**, 13091-13095.
15. M. Vojtek, M. P. M. Marques, I. M. P. L. V. O. Ferreira, H. l. Mota-Filipe and C. Diniz, *Drug Discov. Today*, 2019, **24**, 1044-1058.
16. F. P. Pruchnik, R. Starosta, Z. Ciunik, A. Opolski, J. Wietrzyk, E. Wojdat and D. Dus, *Can. J. Chem.*, 2001, **79**, 868-877.
17. K. R. Dunbar, J. H. Matonic, V. P. Saharan, C. A. Crawford and G. Christou, *J. Am. Chem. Soc.*, 1994, **116**, 2201-2202.
18. A. Koutsodimou and N. Katsaros, *J. Coord. Chem.*, 1996, **39**, 169-197.
19. H. T. Chifotides, K. M. Koshlap, L. M. Pérez and K. R. Dunbar, *J. Am. Chem. Soc.*, 2003, **125**, 10714-10724.
20. H. T. Chifotides, K. M. Koshlap, L. M. Pérez and K. R. Dunbar, *J. Am. Chem. Soc.*, 2003, **125**, 10703-10713.
21. S. U. Dunham, H. T. Chifotides, S. Mikulski, A. E. Burr and K. R. Dunbar, *Biochemistry*, 2005, **44**, 996-1003.
22. D. V. Deubel and H. T. Chifotides, *Chem. Commun.*, 2007, **0**, 3438-3440.
23. S. P. Perlepes, J. C. Huffman, J. H. Matonic, K. R. Dunbar and G. Christou, *J. Am. Chem. Soc.*, 1991, **113**, 2770-2771.
24. C. A. Crawford, J. H. Matonic, W. E. Streib, J. C. Huffman, K. R. Dunbar and G. Christou, *Inorg. Chem.*, 1993, **32**, 3125-3133.
25. E. Rotondo, B. E. Mann, P. Piraino and G. Tresoldi, *Inorg. Chem.*, 1989, **28**, 3070-3073.
26. J. D. Aguirre, D. A. Lutterman, A. M. Angeles-Boza, K. R. Dunbar and C. Turro, *Inorg. Chem.*, 2007, **46**, 7494-7502.
27. A. Enriquez Garcia and F. Jalilehvand, *J. Biol. Inorg. Chem.*, 2018, **23**, 231-239.
28. J. D. Aguirre, H. T. Chifotides, A. M. Angeles-Boza, A. Chouai, C. Turro and K. R. Dunbar, *Inorg. Chem.*, 2009, **48**, 4435-4444.
29. R. A. Howard, T. G. Spring and J. L. Bear, *Cancer Res.*, 1976, **36**, 4402-4405.
30. F.-M. Siu, I. W.-S. Lin, K. Yan, C.-N. Lok, K.-H. Low, T. Y.-C. Leung, T.-L. Lam and C.-M. Che, *Chem Sci.*, 2012, **3**, 1785-1793.

31. J. D. Aguirre, A. M. Angeles-Boza, A. Chouai, J.-P. Pellois, C. Turro and K. R. Dunbar, *J. Am. Chem. Soc.*, 2009, **131**, 11353-11360.
32. B. Peña, R. Barhoumi, R. C. Burghardt, C. Turro and K. R. Dunbar, *J. Am. Chem. Soc.*, 2014, **136**, 7861-7864.
33. M. B. Minus, M. K. Kang, S. E. Knudsen, W. Liu, M. J. Krueger, M. L. Smith, M. S. Redell and Z. T. Ball, *Chem. Commun.*, 2016, **52**, 11685-11688.
34. H. H. Harris, A. Levina, C. T. Dillon, I. Mulyani, B. Lai, Z. Cai and P. A. Lay, *J. Biol. Inorg. Chem.*, 2005, **10**, 105-118.
35. K. L. Munro, A. Mariana, A. I. Klavins, A. J. Foster, B. Lai, S. Vogt, Z. Cai, H. H. Harris and C. T. Dillon, *Chem. Res. Toxicol.*, 2008, **21**, 1760-1769.
36. K. J. Davis, J. A. Carrall, B. Lai, J. R. Aldrich-Wright, S. F. Ralph and C. T. Dillon, *Dalton Trans.*, 2012, **41**, 9417-9426.
37. F. Fus, Y. Yang, H. Z. S. Lee, S. Top, M. Carriere, *et al.*, *Angew. Chem.*, 2019, **131**, 3499-3503.
38. J. B. Aitken, S. Antony, C. M. Weekley, B. Lai, L. Spiccia and H. H. Harris, *Metallomics*, 2012, **4**, 1051-1056.
39. M. J. Pushie, I. J. Pickering, M. Korbas, M. J. Hackett and G. N. George, *Chem. Rev.*, 2014, **114**, 8499-8541.
40. J. Markham, J. Liang, A. Levina, R. Mak, B. Johannessen, P. Kappen, C. J. Glover, B. Lai, S. Vogt and P. A. Lay, *Eur. J. Inorg. Chem.*, 2017, **2017**, 1812-1823.
41. A. Enriquez Garcia, F. Jalilehvand, P. Niksirat and B. S. Gelfand, *Inorg. Chem.*, 2018, **57**, 12787-12799.
42. C. A. Crawford, J. H. Matonic, J. C. Huffman, K. Folting, K. R. Dunbar and G. Christou, *Inorg. Chem.*, 1997, **36**, 2361-2371.
43. A. Z. M. Pauzi, S. K. Yeap, N. Abu, K. L. Lim, A. R. Omar, S. A. Aziz, A. L. T. Chow, T. Subramani, S. G. Tan and N. B. Alitheen, *Chin. Med.*, 2016, **11**, 46.
44. F. Pruchnik and D. Duś, *J. Inorg. Biochem.*, 1996, **61**, 55-61.
45. C. T. Dillon, P. A. Lay, B. J. Kennedy, A. P. Stampfl, Z. Cai, P. Ilinski, W. Rodrigues, D. G. Legnini, B. Lai and J. Maser, *J. Biol. Inorg. Chem.*, 2002, **7**, 640-645.
46. J. L. Wedding, H. H. Harris, C. A. Bader, S. E. Plush, R. Mak, *et al.*, *Metallomics*, 2017, **9**, 382-390.
47. A. M. Angeles-Boza, H. T. Chifotides, J. D. Aguirre, A. Chouai, P. K. L. Fu, K. R. Dunbar and C. Turro, *J. Med. Chem.*, 2006, **49**, 6841-6847.
48. C. M. Weekley, J. B. Aitken, S. Vogt, L. A. Finney, *et al.*, *J. Am. Chem. Soc.*, 2011, **133**, 18272-18279.
49. C. M. Weekley, J. B. Aitken, S. Vogt, L. A. Finney, D. J. Paterson, M. D. de Jonge, D. L. Howard, I. F. Musgrave and H. H. Harris, *Biochemistry*, 2011, **50**, 1641-1650.
50. C. M. Weekley, G. Jeong, M. E. Tierney, F. Hossain, A. M. Maw, A. Shanu, H. H. Harris and P. K. Witting, *J. Biol. Inorg. Chem.*, 2014, **19**, 813-828.
51. F. Jalilehvand, A. Enriquez Garcia and P. Niksirat, *ACS Omega*, 2017, **2**, 6174-6186.
52. M. Pongratz, P. Schluga, M. A. Jakupec, V. B. Arion, C. G. Hartinger, G. n. Allmaier and B. K. Keppler, *J. Anal. At. Spectrom.*, 2004, **19**, 46-51.
53. X.-Y. Yang, J.-Y. Xu, M. Meng, N. Li, C.-Y. Liu and Q.-Y. He, *J. Proteomics*, 2019, **194**, 160-167.